

## Generation of a Population Inversion between Quantum States of a Macroscopic Variable

Siyuan Han, R. Rouse, and J. E. Lukens

*Department of Physics, University at Stony Brook, Stony Brook, New York 11794*  
(Received 13 December 1995)

A population inversion has been created between the two adjacent fluxoid wells (with energy difference  $\varepsilon$ ) in an rf SQUID subject to weak radiation at 100 GHz. The states in the two wells have opposite currents, of magnitude  $\sim 2 \mu\text{A}$ , circulating through an inductance of 0.2 nH. The steady state population of the upper well  $n_u(\varepsilon)$  shows local maxima whose positions correspond to calculated photon absorption resonances between the ground state and an intermediate state. The maximum  $n_u(\varepsilon)$  is 0.94 compared to the expected thermal equilibrium value of  $n_u(\varepsilon) = 2 \times 10^{-9}$ . [S0031-9007(96)00100-7]

PACS numbers: 74.50.+r, 73.40.Gk

Evidence has been obtained which suggests that the quantum effects, e.g., quantized energy levels and tunneling, commonly observed in microscopic systems can also be seen in macroscopic variables ( $\chi$ ) describing the collective motion of a large number of particles. A key to this development has been the understanding of the inevitable effects of the environment on these variables through damping and thermal fluctuations [1]. A current biased Josephson junction ( $\chi$  the junction's phase) and a superconducting loop interrupted by a Josephson junction (a SQUID, with  $\chi$  being the flux linking it) have proven to be good models for both the theoretical and experimental study of the quantum mechanics of macroscopic variables due to their simple structure and high degree of characterization. Both of these systems can be described by potentials with metastable wells. Early experiments showed escape from the wells by tunneling through a barrier [2-4] and energy level quantization within a well [5]. Recent results demonstrate the existence of resonant tunneling between these quantized levels in the macroscopically distinct fluxoid wells of the SQUID potential (MRT) [6]. It has also been predicted that photoinduced transitions between fluxoid wells is greatly enhanced when the energy of photons incident on a SQUID equals the energy difference of states in two wells [7,8]. These effects allow one to envision a maser based on macroscopic quantum transitions. In this Letter, we report an important step in this direction: the generation of a population inversion between the two fluxoid wells of a SQUID.

The system which we use is, effectively, a superconducting loop interrupted by a Josephson junction—commonly known as an rf SQUID. The state of this system can be specified by the applied flux  $\Phi_x$  and the flux  $\Phi$  linking the loop. In the absence of damping this system is described by the Hamiltonian

$$H_0(\Phi, \Phi_x) = \frac{p_\Phi^2}{2C} + U(\Phi, \Phi_x). \quad (1)$$

Here  $C$  is the junction capacitance and  $p_\Phi = -i\hbar\partial/\partial\Phi$ . The potential energy  $U$  of the system is given by

$$U(\Phi, \Phi_x) = \frac{(\Phi - \Phi_x)^2}{2L} + \beta_L U_0 \cos\left(2\pi \frac{\Phi}{\Phi_0}\right), \quad (2)$$

where  $L$  is the inductance of the rf SQUID,  $\beta_L = 2\pi LI_c/\Phi_0$ ,  $I_c$  the junction critical current, and  $U_0 = \Phi_0^2/4\pi^2 L$ . The fluxes  $\Phi$  and  $\Phi_x$  are measured with respect to  $\Phi_0/2$ . This potential, which has been discussed in detail elsewhere [9], is a symmetric double well for  $\Phi_x = 0$  and  $1 < \beta_L < 4.6$  with minima located at  $\Phi = \pm\Phi_m(\beta_L)$ . These wells correspond to fluxoid states with phase winding  $2\pi f$  ( $f$  an integer) of the SQUID differing by  $2\pi$ , e.g.,  $f = 0$  and  $f = 1$ , and are separated by a barrier whose energy  $U_B$ , with respect to the ground state, also depends on  $\beta_L$ . For  $|\Phi_x| \ll \Phi_m$ , the potential tilts linearly in  $\Phi_x$  giving an energy difference  $\varepsilon \approx 2\Phi_m\Phi_x/L$  between the ground states of two fluxoid wells.

The eigenstates of the Hamiltonian, Eq. (1), give typical level structures such as those shown in Fig. 1. There are a series of levels (indexed by  $\{f, i\}$ ) with energies  $E_{f,i}$  less than  $U_B$  which are well localized in either the  $f = 0$  or  $f = 1$  well. The level spacing within a well is approximately  $\hbar\omega_0$ , where  $\omega_0$  is the small oscillation frequency in the well. For our data presented below,  $\hbar\omega_0/k_B \approx 1.4$  K. For energies above  $U_B$ , the level spacing is reduced and

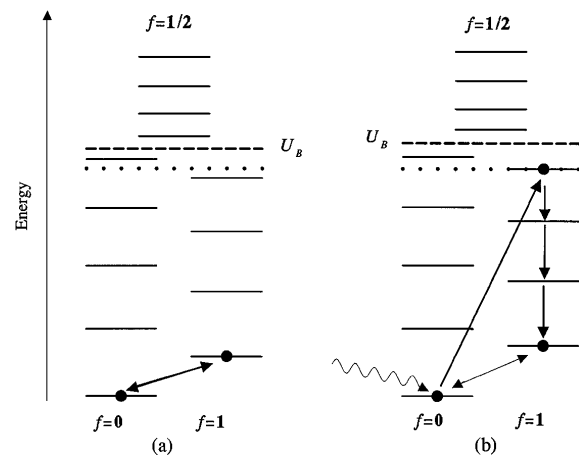


FIG. 1. SQUID energy levels at two different values of  $\varepsilon$  showing the idealized transition paths when the level 1,3 is (a) off the photon absorption resonance and (b) on the resonance. The dotted and dashed lines are the energies of the incident photons and the potential barrier, respectively.

the wave functions for  $\Phi$  are no longer localized in a single fluxoid state. To indicate this delocalization, we index these levels by  $f = \frac{1}{2}$ , e.g.,  $E_{\frac{1}{2},0}$ , realizing that for levels with  $E \approx U_B$  the distinction can become blurred. The level structure within the wells, calculated using this approach with independently determined system parameters, has been found to agree very well with that determined from resonant tunneling data [6]. The real SQUID, of course, also has a source of damping through which the system interacts with the thermal reservoir. For Ohmic damping, this can be modeled as a resistance  $R$  in parallel with the junction. The levels calculated above are sharply quantized when the classical  $Q \equiv RC\omega_0 \gg 1$ , as is the case for the SQUID studied here. In our system, the damping below 1 GHz is dominated by a AuPd foil enclosing the sample SQUID to shield the sample from external perturbations [6] and is equivalent to a shunt resistance of  $R = 4.5 \pm 1.5$  k $\Omega$ . Since  $C \approx 80$  fF,  $Q > 50$  below  $\sim 1$  GHz and increases at higher frequency. In this high- $Q$  limit it has also been shown that the effect of the damping on the level spacing and position is negligible [10,11].

Our approach to the generation of a population inversion is similar to that used in a three level laser. Roughly speaking the system is resonantly pumped from its ground state, in the lower well, to an excited state, at  $E \sim U_B$ , from which it rapidly decays with a substantial probability to the  $i = 0$  level of the upper well where it is then trapped for a relatively long period. In our experiment, the source of photons is the 100 GHz oscillation of the dc SQUID magnetometer, also used to monitor  $\Phi$ . The frequency of these photons is essentially fixed, since significant coupling occurs only at a resonance in the dc transformer coupling the sample and magnetometer. The rf field is quite weak, having been previously determined [6] to have an amplitude  $\Phi_{\text{rf}} < 4 \times 10^{-5}\Phi_0$ . This results in a maximum occupation of the resonant levels of  $n_r < 10^{-6}$ . The values of  $\varepsilon$  and  $\beta_L$ , for which large excess populations of the upper well occur, should be those for which the level spacing between the system's ground state and the pumped (intermediate) state satisfies the resonance condition. An example of the process discussed above is shown in Fig. 1(b). Here the system is resonantly excited from the ground state  $\{0,0\}$  to the level  $\{1,3\}$  in the opposite well from which it rapidly cascades to the  $\{1,0\}$  level. The time for such intrawell decays is roughly  $\tau \sim Q/\omega_0$  [10,11] or on the order of a nanosecond for our system. The lifetime of the  $\{1,0\}$  state against decay to  $\{0,0\}$  is about a millisecond, as extrapolated from the directly measured transition rate for slightly larger  $U_B$  (larger  $\beta_L$ ) [6]. Thus, this process is able to generate a significant excess  $\{1,0\}$  population even with the very weak photon field. In addition to the process shown in Fig. 1(b), pumping to intermediate states in the initial well, e.g.,  $\{0,4\}$ , and above the barrier,  $\{\frac{1}{2},0\}$  and  $\{\frac{1}{2},1\}$ , is also possible.

We determine the population of the upper well from a measurement of the mean flux  $\bar{\Phi}$  linking the SQUID. Since the system temperature is 50 mK for the data presented below,  $k_B T \ll \hbar\omega_0$  and only the lowest level in each well should have a significant population:  $n_u$  ( $n_l$ ) for the upper (lower) well. The mean flux in these levels differs by  $2\Phi_m \approx 0.4\Phi_0$ . Thus, a measurement of the flux linking the SQUID gives the occupation of the two  $i = 0$  levels, i.e.,  $n_u - n_l = -\text{sgn}(\varepsilon)\bar{\phi}(\varepsilon)$ , and  $n_u + n_l = 1$  where  $\bar{\phi}(\varepsilon)$  is the mean flux measured with respect to the average of the mean fluxes of the two wells and normalized to  $\Phi_m$ . This gives the occupation of the upper well in terms of  $\bar{\phi}(\varepsilon)$  to be  $n_u = [1 - \text{sgn}(\varepsilon)\bar{\phi}(\varepsilon)]/2$ . To achieve the steady state, the transition time between the wells must be short compared to the measurement time. This condition is achieved by the variation of the barrier height  $U_B$  *in situ* through the modulation of  $\beta_L$ . The single junction in the model presented above is actually a superconducting loop with a low inductance  $l$  containing two junctions in parallel (a dc SQUID). Since  $2\pi I_c l \ll \Phi_0$ , this is well approximated by a single junction with a critical current that can be modulated by an applied flux  $\Phi_{\text{mod}}$  giving  $\beta_L = \beta_{L0} \cos(\pi\Phi_{\text{mod}}/\Phi_0)$ . For the sample reported here,  $\beta_{L0} = 1.99$ . Since the two junctions in the dc SQUID have critical currents which are equal to better than 1%, the minimum  $\beta_L$  is much less than unity. In thermal equilibrium, the relative occupation of the upper well is just given by the Boltzmann factor, so  $\bar{\phi}(\varepsilon)$  in thermal equilibrium is just  $\bar{\phi}(\varepsilon)_{\text{th}} = \tanh(\varepsilon/k_B T)$ .

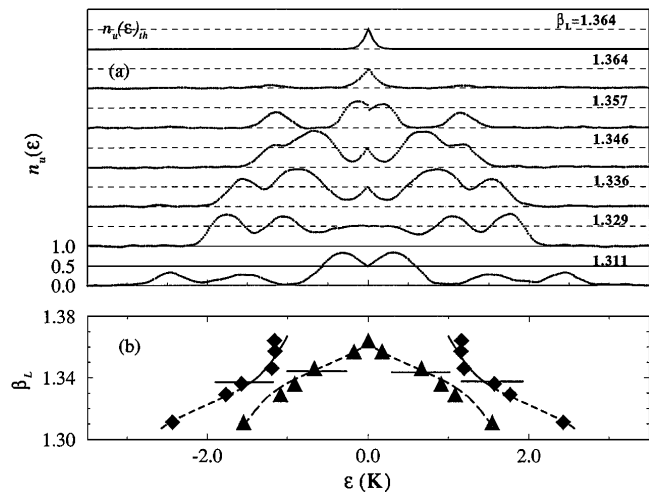


FIG. 2. (a) Upper well population  $n_u$  vs  $\varepsilon$  for different values of  $\beta_L$ . The top curve is the calculated thermal equilibrium population at 50 mK; the rest are experimental data. (b) Squares (triangles) are the position of the outermost (second to the outermost) peaks of  $n_u(\varepsilon)$  vs  $\beta_L$  for the data in (a). The solid, short dashed, and long dashed lines are the position, in  $\varepsilon$ , of calculated photon absorption resonance between the zeroth level of the lower well and an intermediate state in the opposite well, same well, or above the barrier, respectively. The short horizontal lines indicate the boundaries between different types of intermediate states.

The corresponding calculated  $n_u(\varepsilon)_{\text{th}}$ , as shown in the top panel of Fig. 2(a), approaches a maximum value of 0.5 as  $\varepsilon \rightarrow 0$ . In the lower panels of Fig. 2(a), data are presented showing the measured  $n_u(\varepsilon)$  for  $1.311 \leq \beta_L \leq 1.364$ . These data represent the steady state, with the system switching rapidly between wells as  $\varepsilon$  is varied. This is demonstrated by the fact that the measured  $\phi(\varepsilon)$  is independent of the sign of  $d\varepsilon/dt$ . As one can see, the measured data differ dramatically from the predicted  $n_u(\text{th})$ , exhibiting a series of maxima in  $n_u(\varepsilon)$  with values as high as 0.94 for  $\beta_L \approx 1.35$ . This nearly complete inversion of the population represents an occupation of the upper state approximately  $5 \times 10^8$  times the thermal equilibrium value. As  $\beta_L$  is decreased,  $n_u(0)$  periodically changes from a local maximum, as in the equilibrium case, to a local minimum and back. In Fig. 2(b), the calculated potential tilts  $\varepsilon$  are shown (lines) for which a pumping resonance ( $f = 101$  GHz) occurs as a function of  $\beta_L$ . These energy level calculations use the same sample parameters ( $L = 210$  pH,  $\beta_{L0} = 1.99$ , and  $C = 82$  fF) used to fit MRT and photon assisted tunneling data measured for larger  $\beta_L$  [6]. These parameter values also agree well with those independently determined (i.e., not using tunneling data):  $L = 210 \pm 10$  pH,  $\beta_{L0} = 2.00 \pm 0.1$ , and  $C = 80 \pm 25$  fF. As can be seen in Fig. 2(b), the data points, representing the location of the two outermost peaks in  $n_u(\varepsilon)$  for each  $\beta_L$ , are well described by these calculations. These calculated curves are associated with different intermediate states [cf. Fig. 2(b) caption]. The resonant peaks associated with the solid lines in Fig. 2(b) involve a direct photoinduced transition between states in different wells, i.e., between macroscopically distinct states, as depicted in Fig. 1(b). For example, the intermediate state corresponding to the outermost  $n_u$  peaks for  $\beta_L = 1.357$  (Fig. 2) has a >93% probability density in the upper well. These data are the first, indirect evidence for such photoinduced transitions originally predicted by Chakravarty and Kivelson [7,8].

The calculation of the position of the pumping resonances is on a very solid footing since the theory is straightforward and the important sample parameters can be independently determined. In contrast, the calculation of the actual values of  $n_u(\varepsilon)$ , determined by solving the rate master equation for the first 24 levels of the system, is rather approximate since it involves the calculation of the ratio in transition rates with significant uncertainties. In the case of the interwell transitions, complete theories exist only for  $\varepsilon \ll \hbar\omega_0$ , which is usually not the case for our data. These rates, along with the intrawell decay rates, also depend on the damping which can only be estimated over a wide range of frequencies, and on the rf power, for which only the upper limit is known. The intrawell transition rates for dissipation-induced spontaneous decay from level  $\{f, i\}$  to  $\{f, j\}$  are given by [12,13]

$$w_{f,i \rightarrow f,j}^{sp} = \frac{2\pi\delta E}{\hbar} \frac{R_Q}{R} |\phi_{i,j}|^2 \left[ 1 + \coth\left(\frac{\delta E}{2k_B T}\right) \right], \quad (3)$$

where  $\delta E \equiv E_{f,i} - E_{f,j}$  is the energy difference,  $\phi_{i,j}$  is the  $\Phi$  matrix element (normalized to  $\Phi_m$ ) between the levels, and  $R_Q \equiv h/4e^2 = 6.45$  k $\Omega$ . The inverse rates, obtained through detailed balance, are negligible at 50 mK. The photon absorption rates  $w_{f,i \rightarrow g,j}^{ab}$ , both interwell and intrawell, are calculated from Fermi's golden rule with the density of the states of the final level taken to be Lorentzian with a full width  $\gamma \sim (E_{g,j} - E_{g,0})/Q$ . Because of the very low rf power and the resulting small occupation of the intermediate states, simulated emission is also a negligible process compared to spontaneous decay. The spontaneous interwell tunneling rates have been calculated by several authors [14–20]. Since in our system the intrawell decay rate is much greater than the tunnel splitting between levels in the two opposite wells, no coherent oscillation is expected during level crossing. Therefore, the expression given in [18],

$$w_{f,i \rightarrow g \neq f,j}^{sp} = \frac{\Delta^2}{4} \frac{\gamma}{(E_{f,i} - E_{g,j})^2 + \gamma^2/4}, \quad (4)$$

is used for  $i + j \neq 0$ , where  $\Delta$  is the tunnel matrix element between the two interwell levels. The transition rate between levels  $\{0, 0\}$  and  $\{1, 0\}$  is calculated according to the standard incoherent tunneling rate formula for the dissipative two-state system given, e.g., in Refs. [21,22].

The population  $n_u(\varepsilon)$  vs  $\varepsilon$  for the six values of  $\beta_L$ , which correspond to all the data sets in Fig. 2, has been calculated using the sample parameters given above. The calculations reproduce the main features of the data sets. Two of the calculated  $n_u(\varepsilon)$  are shown in Fig. 3, along with the corresponding energy levels, for  $\beta_L = 1.346$  and 1.357. The switching of  $n_u(0)$  from a local maximum to minimum for a change of less than 1% in  $\beta_L$  along

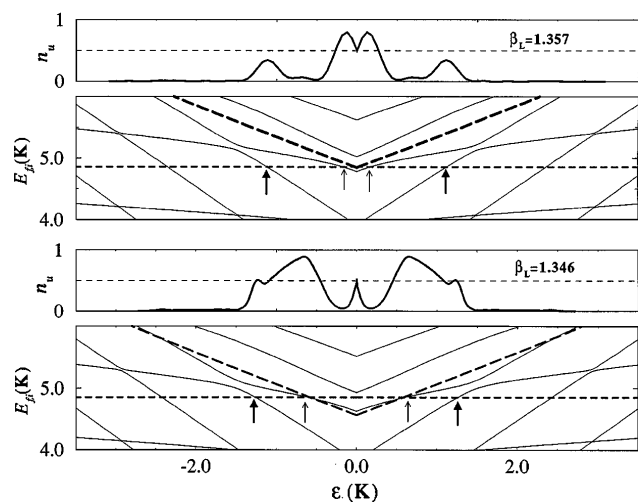


FIG. 3. The calculated upper well population  $n_u$  and the energy levels vs  $\varepsilon$  for two values of  $\beta_L$ . The dark long dashed lines are the energy barriers and the short dashed lines show the energy of the incident photons. The arrows indicate the positions of the photon pumping resonance between the zeroth level of the lower well, to which all energies are referenced, and the intermediate level.

with the structure of the individual curves is reproduced. In our calculation,  $R = 4.5 \text{ k}\Omega$  and  $\Phi_{\text{rf}} = 2 \times 10^{-5} \Phi_0$  were used. The positions, in  $\varepsilon$ , of the  $n_u$  maxima change very little for  $10\mu\Phi_0 \leq \Phi_{\text{rf}} \leq 50\mu\Phi_0$  and  $3 \leq R \leq 6 \text{ k}\Omega$  justifying the more approximate treatment done previously. In contrast, the location of the maxima and the main features of  $n_u(\varepsilon)$  depend very strongly on  $\beta_{L0}$ ,  $L$ , and  $C$  which determine the energy level structure. For instance, increasing  $\beta_{L0}$  by 1% from 1.99 to 2.01 not only shifts the location of the  $n_u$  maximum from  $1\text{m}\Phi_0$  to  $0.2\text{m}\Phi_0$  but also changes  $n_u(0)$  from a local maximum to a local minimum. Thus, the agreement between these features of the data and the calculations using previously determined parameters is quite significant. The deviations of some details of the measured and calculated values of  $n_u(\varepsilon)$  can be attributed to our imprecise knowledge of the damping and rf amplitude as well as the approximate nature of the theory.

In summary, a population inversion has been produced between macroscopically distinct quantum states in different fluxoid wells of a SQUID irradiated with 100 GHz photons. The change in flux between these states is equivalent to a flip in a magnetic moment of  $10^{10} \mu_B$ . The maxima of the population inversion occur when the photon energy equals the energy difference between the ground state of the system and an excited level near the barrier between the fluxoid wells, thus qualitatively giving a macroscopic equivalent to the pumping in a three-level laser. The levels are calculated using system parameters previously determined from measurements of resonant tunneling between the wells and in agreement with independently determined parameters. The magnitude of the upper level population versus applied flux for different barrier heights is well reproduced by solutions to the master equation for transitions among the levels. These results further provide indirect evidence for previously predicted photoinduced transitions between levels in different fluxoid wells.

We wish to acknowledge many useful discussions with D. Averin and A. Garg. In particular, we want to thank K. K. Likharev for his suggestion of methods for creating population inversion and of calculational techniques as well as for his critical reading of the manuscript. This work was supported by the BMDO through the RADC, with initial support from the Office of Naval Research.

- [1] A. Caldeira and A. Leggett, *Ann. Phys. (N.Y.)* **149**, 374 (1983).
- [2] R. F. Voss and R. A. Webb, *Phys. Rev. Lett.* **47**, 265 (1981).
- [3] M. H. Devoret, J. M. Martinis, and J. Clarke, *Phys. Rev. Lett.* **55**, 1908 (1985).
- [4] D. Schwartz, B. Sen, C. Archie, and J. Lukens, *Phys. Rev. Lett.* **55**, 1547 (1985).
- [5] J. M. Martinis, M. H. Devoret, and J. Clarke, *Phys. Rev. Lett.* **55**, 1543 (1985).
- [6] R. Rouse, S. Han, and J. Lukens, *Phys. Rev. Lett.* **75**, 1614 (1995).
- [7] S. Chakravarty and S. Kivelson, *Phys. Rev. Lett.* **50**, 1811 (1983).
- [8] S. Chakravarty and S. Kivelson, *Phys. Rev. B* **32**, 76 (1985).
- [9] S. Han, J. Lapointe, and J. Lukens, in *Activated Barrier Crossing*, edited by G. Fleming and P. Hänggi (World Scientific, Singapore, 1993), 1st ed. Chap. 9, pp. 241–267.
- [10] D. Esteve, M. H. Devoret, and J. M. Martinis, *Phys. Rev. B* **34**, 158 (1986).
- [11] W. Bialek, S. Chakravarty, and S. Kivelson, *Phys. Rev. B* **35**, 120 (1987).
- [12] R. Feynman and F. Vernon, *Ann. Phys. (N.Y.)* **24**, 118 (1963).
- [13] A. Larkin and Y. N. Ovchinnikov, *Sov. Phys. JETP* **64**, 185 (1986).
- [14] N. Hatakenaka, S. Kurihara, and H. Takayanagi, *Phys. Rev. B* **42**, 3987 (1990).
- [15] A. Zhuravlev and A. Zorin, *J. Low Temp. Phys.* **16**, 102 (1990).
- [16] J. Schmidt, A. Cleland, and J. Clarke, *Phys. Rev. B* **43**, 229 (1991).
- [17] Y. Ovchinnikov and A. Schmid, *Phys. Rev. B* **50**, 6332 (1994).
- [18] A. Garg, *Phys. Rev. B* **51**, 15 161 (1995).
- [19] J. Müllers and A. Schmid, *Ann. Phys. (Leipzig)* (to be published).
- [20] Y. Ovchinnikov, P. Silvestrini, B. Ruggiero, and A. Borone (to be published); P. Silvestrini, B. Ruggiero, Y. N. Ovchinnikov, A. Esposito, and A. Barone (private communication).
- [21] M. P. Fisher and A. Dorsey, *Phys. Rev. Lett.* **54**, 1609 (1985).
- [22] A. Leggett *et al.*, *Rev. Mod. Phys.* **59**, 1 (1987).